Available online at www.sciencedirect.com
ScienceDirect
Engineering Structures 30 (2008) 1667–1676
ENGINEERING STRUCTURES
www.elsevier.com/locate/engstruct

Dynamic seismic response of controlled rocking bridge steel-truss piers

Michael Pollino[a,*], Michel Bruneau[b,c]

[a] Simpson, Gumpertz, and Heger Inc., 41 Seyon Street, Bldg. 1, Suite 500, 02453 Waltham, MA, United States
[b] Department of Civil, Structural and Environmental Engineering, University at Buffalo, Buffalo, NY 14260, United States
[c] MCEER, University at Buffalo, Buffalo, NY 14260, United States

Received 27 October 2006; received in revised form 20 October 2007; accepted 22 October 2007
Available online 21 February 2008

Abstract

The dynamic seismic response of steel braced bridge piers allowed to uplift and rock on their foundation is investigated analytically. Allowing piers to rock provides a retrofit solution with increased seismic performance by limiting demands to existing non-ductile elements while damage can be avoided or forced into replaceable structural elements. Also, an inherent restoring mechanism exists that can provide self-centering following an earthquake. However, during the rocking response, as the pier transfers its axis of rotation from the base of one leg to another, the impact and uplift from the foundation excites vertical modes of vibration, increasing the lateral base shear and the axial force demands on the pier legs. Methods are developed to characterize and quantify the increased dynamic demands in order to capacity protect the existing elements. These simplified methods are then compared with the results of nonlinear time history analysis for a set of frames representative of highway bridge piers with aspect ratios of 4, 3 and 2, and shown to be reasonably accurate in most cases. An example set of calculations and analysis results are also presented.
© 2007 Elsevier Ltd. All rights reserved.

Keywords: Steel braced frames; Seismic response; Rocking; Retrofit; Bridges

1. Introduction

The reliance on stable rocking to provide satisfactory seismic performance has recently received a renewed interest: more research is being conducted on this topic and various levels of rocking response have been considered in the retrofit of large bridges. This is in part due to a growing appreciation for the ability of such systems to efficiently withstand seismic demands elastically with little to no damage while providing a self-centering ability. As part of the ongoing research on the topic, Pollino and Bruneau [1] have proposed a controlled rocking system for bridge steel-truss piers where passive energy dissipation devices are added at the base of the structure to control the response of a rocking system otherwise free to uplift. The devices are designed to limit demands to the structure such that it can remain elastic and all damage is forced into these easily replaceable structural "fuses". However, in order to ensure that such rocking structures remain elastic, the maximum forces expected to develop must account for all dynamic effects in the system during the rocking response. Once the designer is able to reliably predict the maximum forces expected to develop within the structure during the rocking response, all members and connections can be designed to remain elastic.

A methodology to quantify the dynamic force effects is presented for a simple steel bridge braced frame. However, the concepts presented are general and could be extended to include different materials and structural systems. The steel braced frame considered is illustrated in Fig. 1 and has a number of square panels (n) with a height (h) and a width ($d = h/n$) with the bracing members in a concentric X-configuration. For this bridge application, all system mass is lumped at the top of the frame legs, as shown in Fig. 1. The predicted response of the proposed controlled rocking concept is then compared with the results of nonlinear dynamic time history analysis for a set of frames representative of bridge steel truss piers having aspect ratios (h/d) of 4, 3, 2 and for a range of energy dissipating device properties. A more detailed example is also shown to illustrate the process of predicting maximum forces and to provide a sample set of results.

* Corresponding author. Tel.: +1 781 907 9373; fax: +1 781 907 9009.
E-mail address: mcpollino@sgh.com (M. Pollino).

0141-0296/$ - see front matter © 2007 Elsevier Ltd. All rights reserved.
doi:10.1016/j.engstruct.2007.10.016

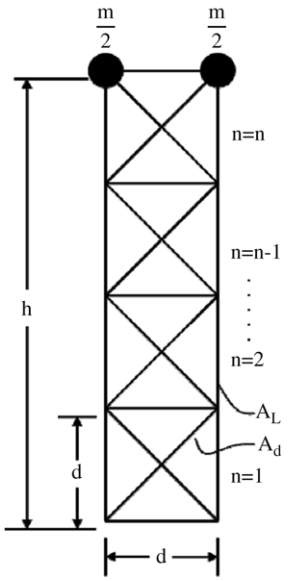

Fig. 1. Simplified steel-braced frame.

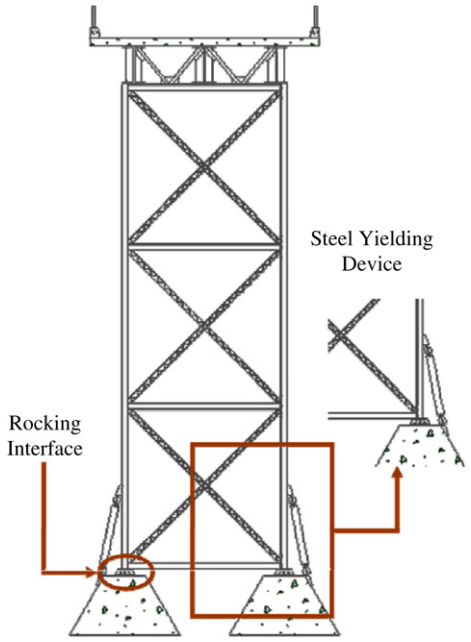

Fig. 2. Retrofitted bridge steel-truss pier using controlled rocking approach.

2. Prior relevant research

The study of rocking structures is not new and Housner [2] first investigated the free and forced vibration response of rigid rocking blocks. Assuming an inelastic impact to occur during each half-cycle, Housner developed equations for the reduction in energy resulting from each impact by equating the moment of momentum and determining the reduction in velocity following the impact. Meek [3] introduced aspects of structural flexibility to the seismic response of single-degree-of-freedom (SDOF) rocking structures and Psycharis [4] followed with an analytical study of the dynamic behaviour of simplified multi-degree-of-freedom (MDOF) structures supported on flexible foundations free to uplift. It was noted in the latter study that vertical oscillations were introduced to this uplifting system even when subjected solely to horizontal excitation.

A number of experimental studies have also been conducted on rocking structural systems. Priestley et al. [5] tested a simple SDOF model investigating its response in free vibration, to sinusoidal input, and to the horizontal component of the 1940 El Centro earthquake. Results showed a significant fluctuation in horizontal acceleration during rocking and large vertical accelerations were induced during impact. Midorikawa et al. [6] experimentally examined the response of a steel-braced frame that allowed uplifting at the base of columns and yielding of specially designed base plates. The shaking table tests solely used horizontal seismic base excitation and it was observed that "the maximum axial forces of columns may be affected by the impact with landing of base plate".

Thus, past analytical and experimental studies investigating systems that allow a rocking response have observed the increased demands placed on structural systems due to dynamic effects. However, they have not provided significant insight into the possible mechanisms causing these additional demands and on design methods to reliably account for their magnitude for steel-braced frames. As part of a capacity-based design philosophy, to capacity protect the primary structural elements of the system during seismic excitation, these demands must be accounted for.

Some of the earliest structures designed and constructed to allow a rocking response during seismic excitation include the South Rangitikei Rail Bridge and an industrial chimney at the Christchurch Airport, both in New Zealand [7]. The north approach of the Lions' Gate Bridge in Vancouver, British Columbia was upgraded in the 1990s with a seismic resistance strategy allowing the steel bridge piers (braced frame) to uplift and rock on their foundations [8]. Some concerns arose due to the effects of dynamic impacting of the pier legs with the foundation and coupling of horizontal and vertical modes during rocking. Dynamic, nonlinear 3-dimensional time history analysis was used to assess the dynamic effects. Some major bridges in California have also allowed at least partial uplift of pier legs as a means of providing satisfactory seismic performance, including the Carquinez [9], San Mateo-Hayward [10], and Golden Gate Bridges [11].

Studies on the controlled rocking approach, presented in [1], included development of the static hysteretic behaviour using step-by-step plastic analysis concepts, simplified methods of analysis for design, a design method for calibration of the passive energy dissipation devices and results of time history analyses. The design procedure includes a set of design constraints that provides limits on response such as preventing excessive displacements and overturning. It was demonstrated that preventing overturning of a frame of significant size, such as a bridge pier, can be easily achieved. A sketch of a bridge pier retrofitted using such an approach is shown in Fig. 2. The passive energy dissipation device considered is a steel yielding device that is assumed to exhibit elastic–perfectly plastic hysteretic behaviour with a yield force, P_{yd}, an elastic stiffness, k_{yd} and a yield displacement, Δ_{yd}. The strength of the steel-yielding device is expressed as a fraction of the frame

tributary vertical weight (w) such that:

$$P_{yd} = \eta_L \cdot \frac{w}{2} \tag{1}$$

where η_L is termed the local strength ratio. This paper provides additional fundamental knowledge on the dynamic response of controlled rocking frames, building from concepts presented in [1] by formulating equations to quantify the forces that develop in the frame during rocking response in a manner amenable for design.

3. Static transfer of loads

Before addressing the dynamic response of rocking steel-braced frames, it is worthwhile to briefly review their static behaviour. The transfer of loads statically through the braced frame during rocking response is described for a half-cycle of motion (shown in Fig. 3) starting from a displacement of $-\Delta_u$ (position 1 in Fig. 3), a point at which one side of the frame has uplifted from the foundation and yielded the steel device. The free body diagram of the frame in five different positions while rocking (assuming static response) from left to right, is shown in Fig. 3. As the frame travels from position 1 to 2, the force in the steel device is reversed and the steel device yields until the uplifted leg returns to its support at position 2. In position 2, half of the weight, $w/2$, is being transferred directly down the left leg while a portion of the weight, $w/2(1-\eta_L)$, is transferred through the frame diagonals also to this leg. From 2 to 3 the portion of the weight, $w/2(1-\eta_L)$, is transferred to the impacting leg on the right. From 3 to 4 the frame begins to move in the other direction and the other half of the weight, $w/2$, is transferred to the leg on the compressive side through the diagonals. At position 4, the frame is on the verge of uplift and then from 4 to 5 the frame uplifts, activating the steel device until it reaches its yield force ($\eta_L w/2$) at point 5. This force is transferred through the frame vertically to the compressive side. One complete hysteretic cycle is also seen in Fig. 3 and the system is shown to develop "flag-shaped" hysteretic behaviour. A more complete description of the hysteretic behaviour (including the difference in response between the first and subsequent cycles) is discussed in Pollino and Bruneau [1].

4. Dynamic response of controlled rocking frame

If the system is designed to allow for frame rocking and self-centering, then after a leg uplifts from the foundation, it eventually returns to its support with a certain velocity upon impact (position 2 in Fig. 3). An energy balance of the frame is applied from positions 1 (maximum displacement) to 2 in order to determine the maximum impact velocity of the pier leg including the plastic work done by the energy dissipating devices in this application. Without a more sophisticated analysis of the impact that occurs between the frame leg and the foundation, an elastic impact is assumed to occur resulting in no loss of system energy thus providing an upper bound on the forces developed within the frame. As the frame leg begins the impacting process, the weight tributary to that leg

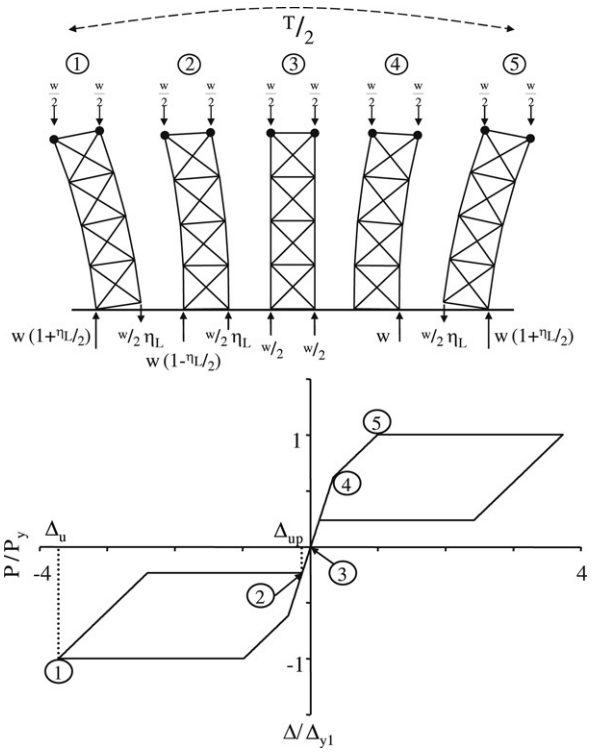

Fig. 3. Static free-body diagrams and hysteretic response of frame through half-cycle of rocking motion.

is also suddenly (impulsively) returned to the impacting leg forcing the leg to remain in contact with the foundation. As the motion continues, the frame shifts its axis of rotation from the base of one leg to another and the weight and device forces are suddenly transferred through the frame vertically to the frame leg that is now being compressed. Beginning with the initial velocity upon impact and followed by the transfer of impulsive forces, a number of dynamic effects are occurring that need to be considered to capacity protect the frame. A fundamental structural dynamics approach is used here that identifies the vertical modes of vibration that are excited and calculates the response from each dynamic effect when the frame is subjected to horizontal excitation. As will be shown, the forces developed due to the vertical accelerations of the mass can be quite significant and need to be accounted for to achieve capacity protection of the frame.

5. SDOF elastic systems subjected to impulsive load

Since the controlled rocking approach assumes the existing frame to be a capacity-protected system, such that it remains linear elastic, the vertical modes excited during impact and uplift are evaluated separately using simplified linear mass–spring systems. Dynamic effects are then superimposed to obtain total response of the rocking frame system.

The response of a SDOF undamped linear mass–spring system subjected to a step force with maximum force, p_o, and finite rise time, t_r, is discussed first to summarize the relevant theory used here to determine the dynamic amplification caused by the impulsive loads transferred through the frame during the rocking response. Including damping in the analysis of

the dynamic response of the frame has little influence since the dynamic forces reach a maximum before damping has a significant effect. The form of applied load can be defined as:

$$p(t) = p_o \frac{t}{t_r} \quad (t \le t_r)$$
$$p(t) = p_o \quad (t \ge t_r) \tag{2}$$

A general solution for the displacement response of this simplified system, subjected to the form of loading described with zero initial conditions, can be easily determined by formulating the equations of motion of the SDOF mass–spring system and solving [12] such that:

$$u(t) = (u_{st})_o \left(1 - \frac{1}{\omega_n t_r}[\sin \omega_n t - \sin \omega_n (t - t_r)]\right) \quad (t \ge t_r)$$
$$u(t) = (u_{st})_o \left(\frac{t}{t_r} - \frac{\sin \omega_n t}{\omega_n t_r}\right) \quad (t \le t_r) \tag{3}$$

where ω_n is the natural frequency of the mass–spring system, $(u_{st})_o$ is the static displacement response of the system subjected to the same maximum force, p_o, and is defined as:

$$(u_{st})_o = \frac{p_o}{k} \tag{4}$$

where k is the stiffness of the spring in the simple spring-mass system. A dynamic amplification factor, R_d, defined as the ratio of maximum displacement response over time, u_o (maximum of Eq. (3)), to the static displacement response (Eq. (4)) can be shown to equal:

$$R_d = \frac{u_o}{(u_{st})_o} = 1 + \frac{\left|\sin\left(\frac{\pi t_r}{T_n}\right)\right|}{\frac{\pi t_r}{T_n}} \tag{5}$$

Therefore the dynamic amplification factor is dependent only on the rise time of the applied load (t_r) and natural period of the mass–spring system representing the vertical mode of vibration (T_n). Also, since the system is linear, forces are directly proportional to deformations; thus R_d also defines the ratio of maximum force response to the static force response. In other words, the maximum force can be determined by amplifying the static force by R_d.

If the same linear mass–spring system were subjected solely to an initial velocity, v_o, the time varying displacement response could simply be defined as

$$u(t) = \frac{T_n v_o}{2\pi} \sin\left(2\pi \frac{t}{T_n}\right) \tag{6}$$

6. Simplified mass–spring systems

6.1. Axial mode of frame legs

As described above, as the frame steps from one leg to another, a series of loads are transferred through the frame vertically. A number of behaviours described in this section start when the leg impacts the foundation with a vertical velocity, v_o, and a portion of its tributary weight, $w/2(1-\eta_L)$, is re-applied to the leg. Thus, the first simple mass–spring system investigated represents the axial vibration of a leg with mass concentrated at the top of the leg, as shown in Fig. 4(a). The stiffness of this system can be taken as

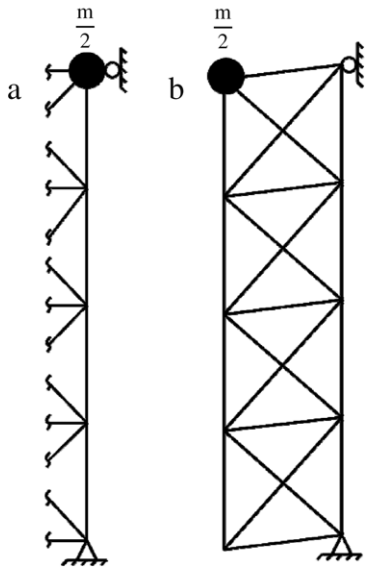

Fig. 4. Frame behaviour representing simplified mass–spring systems.

$$k_L = \frac{E A_L}{h} \tag{7}$$

where A_L is the cross-sectional area of a leg and h is the total height of the leg. The system mass is assumed to only consist of the concentrated mass, $m/2$, at the top of the leg, therefore the period of vibration can be taken as:

$$T_L = 2\pi \sqrt{\frac{m}{2k_L}} \tag{8}$$

As the motion continues from position 2 to 3 (Fig. 3), half of the frame's tributary vertical weight is transferred directly down the frame leg. This impulsive load can be defined by Eq. (2). To determine the effect of the impulsive load, an approach to approximate the rise time of the impulsive load is required. The approach is based on free-vibration response of the frame approximating its primary horizontal rocking mode as a linear elastic system and assuming equivalent response times between the two systems. The response of the equivalent linear elastic system with respect to time can be expressed as:

$$\Delta(t) = \Delta_u \sin\left(2\pi \frac{t}{T_{\text{sec}}}\right) \tag{9}$$

where Δ_u is the maximum global horizontal displacement of the frame (and could be determined using methods described in Pollino and Bruneau [1]) and T_{sec} is the secant period of vibration taken at the maximum system displacement such that:

$$T_{\text{sec}} = 2\pi \sqrt{\frac{m \Delta_u}{P_y}} \tag{10}$$

where P_y is the horizontal yield force of the controlled rocking system and can be determined using the free-body diagram in position 5 of Fig. 3 and shown to equal:

$$P_y = (1 + \eta_L)\frac{w}{2}\frac{d}{h} \tag{11}$$

Therefore the time it takes the system to travel from position 2 to 3 (Fig. 3) is defined as the rise time for the load applied directly down a leg, t_{rL}, and can be approximated by the expression:

$$t_{rL} = \frac{T_{\text{sec}}}{2\pi}\sin^{-1}\left(\frac{\Delta_{\text{up}}}{\Delta_u}\right) \tag{12}$$

where Δ_{up} is the horizontal displacement of the frame at the point of uplift. Finally, the dynamic amplification factor for this load, R_{dL}, can be defined by:

$$R_{dL} = 1 + \frac{\left|\sin\left(\frac{\pi t_{rL}}{T_L}\right)\right|}{\frac{\pi t_{rL}}{T_L}} \tag{13}$$

Since this load acts through the new axis of rotation, it does not affect the base overturning moment. However, it will affect the maximum axial force developed in the leg.

6.2. Vertical shear mode of frame

As the rocking motion continues, vertical loads are transferred through the frame vertically to the other side as the frame uplifts. During uplift the simple mass–spring system is assumed to be subjected to zero initial conditions unlike during impact. Two loads are applied in series during uplifting (positions 3 to 5, Fig. 3). First, a load of $w/2$ is transferred through the frame vertically as the gravitational restoring moment is overcome followed by the yield force of the device.

The vertical stiffness in shear of the system for frames with panel heights equal to the frame width and diagonals in an X-braced configuration could be taken as

$$k_v = \left(\frac{5h}{8EA_L} + \frac{\sqrt{2}d^2}{2hEA_d\cos^2\theta}\right)^{-1} \tag{14}$$

where E is the modulus of elasticity of steel, A_d is the cross-sectional area of the frame diagonals, A_L is the cross-sectional area of the frame legs, h is the frame height, d is the frame width, and θ is the angle the diagonals make with the horizontal. For the vertical shearing mode of vibration shown in Fig. 4(b), the effective mass is taken equal to $m/2$. The period of vibration of this simplified system is therefore

$$T_v = 2\pi\sqrt{\frac{m}{2k_v}} \tag{15}$$

This expression does not account for the minor participation of the mass from the remaining vertical tributary mass of the frame. Performing elastic modal analysis of a system as depicted in Fig. 4(b) including mass from both sides would more accurately determine the period of this mode however this difference does not significantly change the maximum developed forces. For simplicity in design, Eq. (14) could be used.

As the frame moves from position 3 to 5, the two uplifting forces ($w/2$ and P_{yd}) are transferred through the frame vertically with different rise times. The complexity of considering the two separate loads and superposition of their individual dynamic amplification including phase differences is not warranted with the simplified systems used. Therefore an approach is taken to obtain a single amplification factor for the two uplifting loads. Following that approach, a rise time, t_{rv}, is defined for the two loads during uplift as:

$$t_{rv} = \frac{T_{\text{sec}}}{2\pi}\sin^{-1}\left(\frac{\frac{1}{2}\Delta_{y1}}{\Delta_u}\right) \tag{16}$$

where Δ_{y1} is the frame displacement at the point of yield. Therefore the dynamic amplification factor for the sum of these two loads is taken as

$$R_{dv} = 1 + \frac{\left|\sin\left(\frac{\pi t_{rv}}{T_v}\right)\right|}{\frac{\pi T_{rv}}{T_v}} \tag{17}$$

7. Demands on frame legs and frame diagonals by impact and impulsive loads

Using the concepts presented above, member demands can be determined using frame free-body diagrams that include the dynamic loads as shown in Fig. 5. Applying the dynamic amplification factor R_{dv} to the loads transferred during uplift also lead to fluctuation in the horizontal shear demand (due to dynamic moment equilibrium). Therefore, an "effective" static shear can be used to evaluate the adequacy of the frame's lateral load path by amplifying the static frame yield force (Eq. (11)) by R_{dv} such that the ultimate base shear demand can be expressed as:

$$P_u = \frac{w}{2}\frac{d}{h}(1 + \eta_L)R_{dv} \tag{18}$$

where R_{dv} is defined by Eq. (17). Limiting the device strength, P_{yd}, to an acceptable level or strengthening of the weak elements along the lateral load path is required to prevent damage to the frame.

Conservatively estimating the ultimate load on the legs is essential because they resist the gravity loads. As was discussed, the maximum axial force in a leg is a result of the impacting as the leg returns to its support, followed by the impulsive application of a portion of its tributary weight, and the loads transferred through the diagonals as uplift occurs in the other direction.

7.1. Impact force on leg

The maximum dynamic force demand due to the initial velocity upon impact, P_{vo}, is taken equal to:

$$P_{vo} = k_L u_{vo} = k_L\frac{v_o T_L}{2\pi} = v_o\sqrt{\frac{mk_L}{2}} = v_o\sqrt{\frac{mEA_L}{2h}} \tag{19}$$

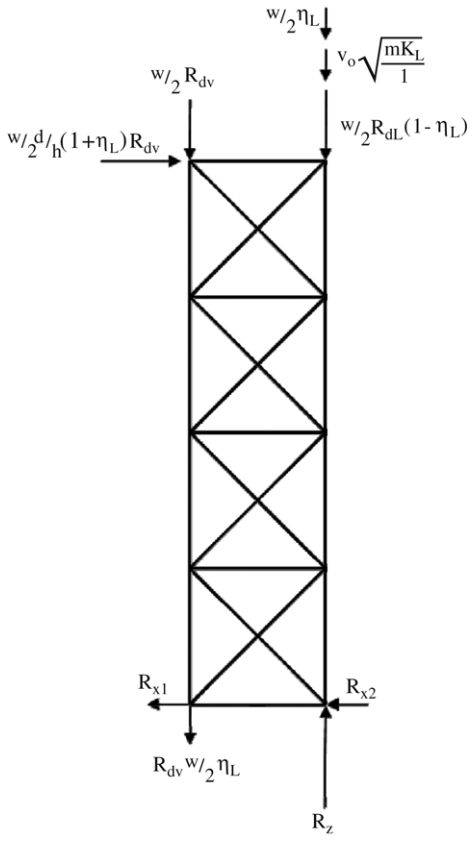

Fig. 5. Dynamic free-body diagram of frame.

where the term, u_{vo}, is the maximum displacement caused by the initial velocity upon impact (from Eq. (6)).

The velocity upon impact could be determined using an energy balance approach where energy is equated at the point of maximum deformation (position 1 in Fig. 3) and just before the point of leg impact with the support (position 2 of Fig. 3) with the energy dissipated by the yielding device included as work done between these two points. The energy balance would be defined as:

$$PE_1 + KE_1 + W_{1-2} = PE_2 + KE_2 \tag{20}$$

where the kinetic energy at position 1 (KE_1) is equal to zero since the frame is at the maximum deformation and has zero velocity. The potential energy at position 1 (PE_1) includes the internal strain energy developed in the frame members, gravitational potential energy of the mass as the leg is uplifted, and strain energy in the steel yielding device such that:

$$PE_1 = \frac{1}{2}\frac{P_y^2}{k_o} + \Delta_{upL}\frac{w}{2} + \frac{1}{2}\left(\frac{w}{2}\eta_L\right)\Delta_{yd} \tag{21}$$

where k_o is the frame lateral stiffness and Δ_{upL} is the maximum uplift displacement of a leg and can be related to the maximum displacement of the frame. The work done by the steel yielding device from position 1 to 2 is equal to:

$$W_{1-2} = P_{yd}(\Delta_{upL} - 2\Delta_{yd}) \tag{22}$$

The potential energy at position 2 (PE_2) includes a smaller amount of strain energy in the frame members (as opposed to position 1) and no gravitational potential energy as the leg has returned to the support such that:

$$PE_2 = \frac{1}{2}\frac{\left[(1-\eta_L)\frac{w}{2}\frac{d}{h}\right]^2}{k_o} \tag{23}$$

Finally, the kinetic energy at position 2 (KE_2) can be related to the vertical leg velocity as:

$$KE_2 = \frac{1}{2}mv_o^2\left[\left(\frac{h}{d}\right)^2 + \frac{1}{2}\right] \tag{24}$$

Placing Eqs. (21)–(24) into Eq. (20) and solving for v_o results in:

$$v_o = \sqrt{g\left(\frac{1}{\frac{1}{4}\left(\frac{h}{d}\right)^2 + \frac{1}{2}}\right)\cdot\left[\frac{w}{2}\frac{\eta_L^2 - 1}{k_o}\left(\frac{d}{h}\right)^2 + 2\eta_L\Delta_{yd} + \Delta_u\frac{d}{h}(1-\eta_L)\right]} \tag{25}$$

This approach does not take into account work done by the ground motion during the time the frame displaces from position 1 to 2. This could be considered the inelastic pseudo-velocity of the controlled rocking system as is similarly defined for elasto-plastic systems [13].

7.2. Transfer of gravity and device forces

From position 1 to 2, the axial force in the leg that will impact the support reverses load from tension to compression ($\eta_L w/2$) as a result of the yielding device. As the motion of the frame continues from position 2 to 3, a portion of the tributary weight is impulsively applied to the leg. This demand, P_{wL}, is determined by applying the dynamic amplification factor R_{dL}, defined by Eq. (13), such that:

$$P_{wL} = R_{dL}\frac{w}{2}(1-\eta_L) + \frac{w}{2} \tag{26}$$

The maximum demand in the 1st panel leg, due to the loads transfer through the frame as it uplifts and yields the device, P_v, is:

$$P_v = P_u\frac{h}{d}\left(1 - \frac{d}{2h}\right) = \frac{w}{2}(1+\eta_L)R_{dv}\left(1 - \frac{d}{2h}\right) \tag{27}$$

These loads include the static demands along with the maximum expected dynamic effects (assuming they are all in-phase). However, the dynamic effects that are a result of excitation of vertical modes do not all oscillate at the same frequency and are excited at different times therefore are out of phase. Using Eqs. (3) and (6), the response due to each load could be superimposed to determine the total response. However, it is simpler and sufficient to use combination rules to combine the maximums of each response. A conservative estimate would be found using an absolute sum (ABS) rule, but using a square-root-sum-of-squares (SRSS) or complete-quadratic-combination (CQC) combination rule [14] may be more appropriate.

8. Example — Bridge Pier with $h/d = 4$

The methods described above, for determining the maximum dynamic forces are illustrated using an example frame with properties representative of a bridge steel-truss pier. The steel-truss pier investigated has an aspect ratio (h/d) of 4 with a width of 7.32 m and thus a height of 29.26 m and diagonals in an X-braced configuration. The cross-sectional area of the pier leg, A_L, is taken equal to 310 cm^2 while the area of a single pier diagonal, A_d, is taken equal to 71 cm^2. The "fixed-base" lateral stiffness of the pier, k_o, is equal to 12.6 kN/mm. The steel yielding device has a yield force, P_{yd}, equal to $w/4$ ($\eta_L = 0.50$), an elastic stiffness, k_{yd}, of 175 kN/mm and its yield displacement, Δ_{yd}, is equal to 2.47 mm. An equivalent mass is assumed to act in the horizontal and vertical directions, equal to:

$$m = \frac{w}{g} = \frac{1730\ \text{kN}}{9.81\ \text{m/s}^2} = 176.4\ \text{kN s}^2/\text{m} \tag{28}$$

The stiffness of the two simplified, linear mass–spring systems described previously can now be determined. First the axial stiffness of a pier leg can be determined from Eq. (7) and the axial period of vibration (Eq. (8)) is equal to 0.13 s. The vertical shear stiffness of the pier is determined from Eq. (14) and the vertical shearing mode of vibration has a period (Eq. (15)) equal to 0.13 s. From elastic modal analysis, the value of T_v is found to be 0.16 s.

The rise time for $w/2(1-\eta_L)$ being applied directly down a pier leg, t_{rL}, is determined using Eq. (12). Using a typical response spectra for bridge design [14], with the spectral acceleration given in 8.1 and methods presented in [1], the ultimate global pier displacement, Δ_u, and the displacement at the point of uplift can be determined. The rise time for the impacting load is found to be:

$$\begin{aligned} t_{rL} &= \frac{T_{\text{sec}}}{2\pi}\sin^{-1}\left(\frac{\Delta_{\text{up}}}{\Delta_u}\right) \\ &= \frac{1.6\ \text{s}}{2\pi}\sin^{-1}\left(\frac{17.1\ \text{mm}}{165\ \text{mm}}\right) = 0.026\ \text{s} \end{aligned} \tag{29}$$

and similarly for the loads applied vertically through the truss pier, t_{rv} (Eq. (16)) is equal to 0.05 s. The amplification factors can now be determined using Eqs. (13) and (17):

$$R_{dL} = 1 + \frac{\left|\sin\left(\frac{\pi t_{rL}}{T_L}\right)\right|}{\frac{\pi t_{rL}}{T_L}} = 1 + \frac{\sin\frac{\pi\cdot(0.026\ \text{s})}{0.128\ \text{s}}}{\frac{\pi\cdot(0.026\ \text{s})}{0.128\ \text{s}}} = 1.93 \tag{30}$$

and similarly, R_{dv} can be shown equal to 1.77.

The maximum dynamic base shear from Eq. (18) is:

$$\begin{aligned} P_u &= \frac{w}{2}\frac{d}{h}(1+\eta_L)R_{dv} = \left(\frac{1730\ \text{kN}}{2}\right)\frac{1}{4}(1+0.5)1.77 \\ &= 574\ \text{kN} \end{aligned} \tag{31}$$

The pier leg impact velocity, v_o, is equal to 208 mm/s following the energy approach (Eq. (25)). The pier leg dynamic demands defined by Eqs. (19), (26) and (27) are determined to be 900 kN, 1270 kN, and 2010 kN respectively. Using an SRSS combination of the dynamic effects, the maximum pier leg axial force is equal to 2540 kN.

8.1. Comparison with nonlinear time history analysis

An analytical model is developed to more accurately determine the response of the controlled rocking frame. Elastic frame elements are used to model frame legs and diagonals. Rocking at the foundation is modelled using a compression-only gap element in parallel with a bilinear hysteretic model proposed by Wen [15]. Restraints are also provided at this location to transfer the horizontal shear forces at the base (thus assuming that sliding is prevented) but provide no resistance to vertical movements. Equal inertial mass is applied in the horizontal and vertical directions at two discrete points at the top of each frame leg as shown previously. A Rayleigh damping matrix is used with 2% damping assigned to periods of approximately $1.5T_o$ (fixed-base period of pier) and 1/4 times the smaller of T_L or T_v. The use of a Rayleigh damping matrix in the time history analyses has minor influence due to the low levels of damping inherent in the structure, however, assists in the numerical solution by damping out localized higher modes of vibration. As discussed previously, this simplified model was used to verify the concepts presented using a general approach that could be expanded upon and applied to other structural systems and materials.

Spectra compatible ground acceleration time histories are used for the dynamic analyses and are generated using the Target Acceleration Spectra Compatible Time Histories (TARSCTHS) software developed by the Engineering Seismology Laboratory (ESL) at the University at Buffalo and is the implementation of the method described in [16]. The elastic response spectral shape is defined by NCHRP 12-49 [14] with a design one-second spectral acceleration value (S_{D1}) of $0.5g$ and a design short period spectral acceleration value (S_{DS}) assumed equal to 2.5 times S_{D1}. This results in a characteristic period, T_s, of 0.4 s, typical of a rock site.

A single spectra compatible motion is used to assess the results for the example of a bridge pier with aspect ratio of 4. Global pier relative displacement is shown in Fig. 6(a) along with the uplifting displacement of the two legs. The recentring ability of the system is evident from the pier relative-displacement result. The global pier hysteretic behaviour is shown in Fig. 6(b). The dotted line shown in the figure is response of the same analytical model to the same excitation except that no vertical inertial mass is included in the model. The fluctuation of the base shear response is evident especially as the pier undergoes significant displacement excursions. The base shear with respect to time is plotted in Fig. 6(c) and the leg axial forces shown in Fig. 6(d). The increased dynamic response, due to the oscillation of vertical modes, is shown in each figure and the frequency of the oscillations approximately equal to the calculated values.

9. Parametric study

Results of a small parametric study are presented for braced frames that are representative of bridge steel-truss piers with

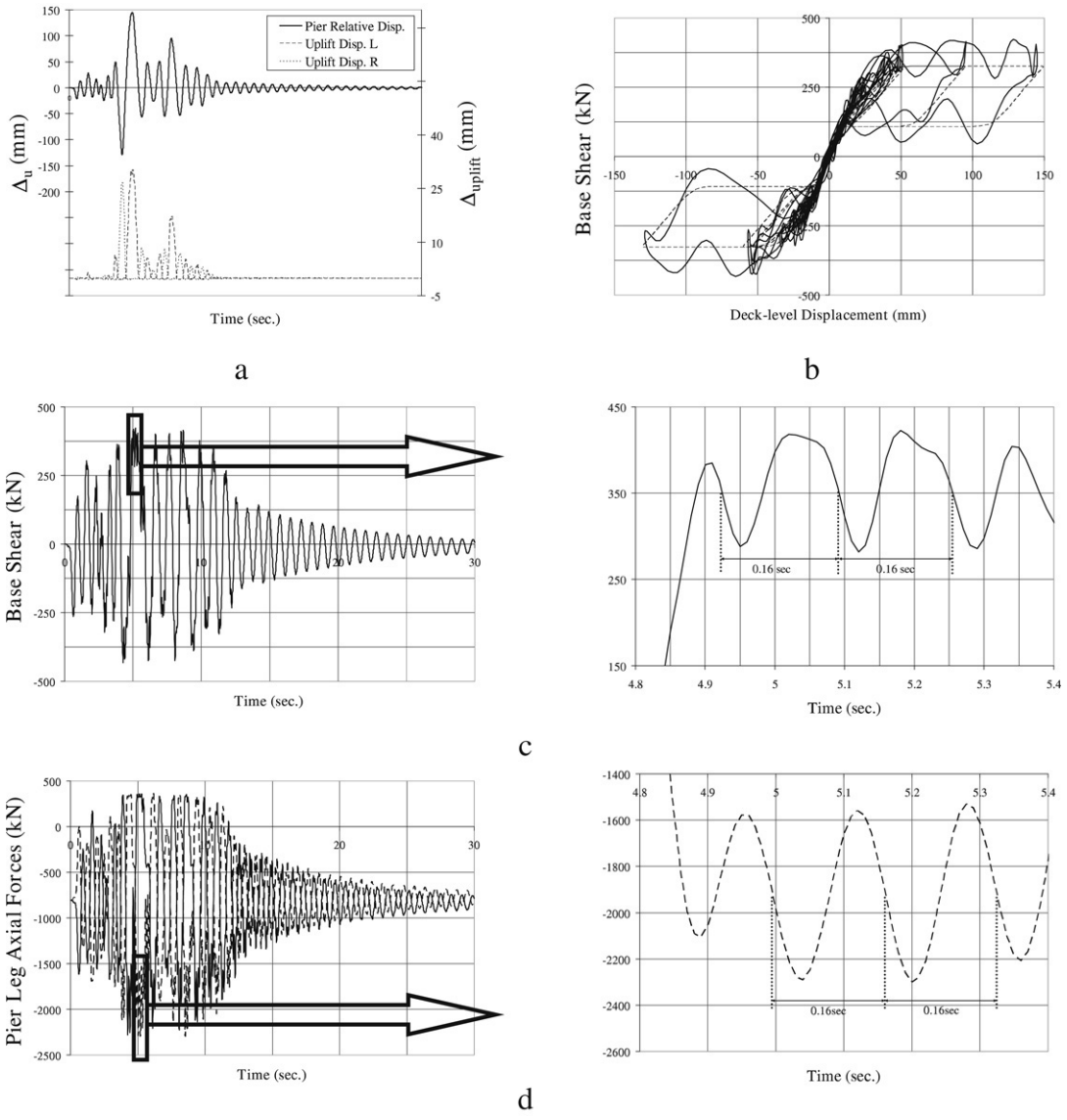

Fig. 6. Results of dynamic analysis — Example (a) pier relative displacement and uplifting displacements of two legs, (b) global hysteretic response, (c) horizontal base shear, and (d) leg axial forces.

aspect ratios (h/d) of 4, 3, and 2; steel devices with local strength ratios (η_L) of 0, 0.25, 0.50, 0.75, 1.0; and an effective rocking period of vibration ratio (T_{eff}/T_o) defined in [1] of 1.0, 1.25, and 1.5. The cross-sectional area of the legs and diagonals are the same for all frames. Likewise, the horizontal and vertical tributary masses (and gravitational loads) are assumed to be the same. The frames are of the same width, and their height changes accordingly with the aspect ratio. The resulting relevant dynamic properties for all aspect ratios considered are shown in Table 1.

The parametric study uses nonlinear time history analysis to assess the concepts presented for a larger range of possible design solutions for the controlled rocking seismic resistance strategy. The analytical models used in the parametric study are identical to that used in the example except that the frame aspect ratios and device properties are changed as dictated by the parameters. A set of seven synthetic ground motions are used that are generated to match the same design spectrum used in the example.

Table 1
Relevant dynamic properties of each aspect ratio

h/d	T_L (s)	T_v (s)
4	0.128	0.155
3	0.111	0.141
2	0.091	0.139

The mean result of the seven synthetic ground motions is shown for each case considered. A total of 39 cases were considered, and thus 273 analyses were performed. Results are presented in Fig. 7 for the maximum base shear ($P_{u,TH}$) and maximum leg axial force ($P_{uL,TH}$) normalized by the values determined using the concepts above for each system parameter considered.

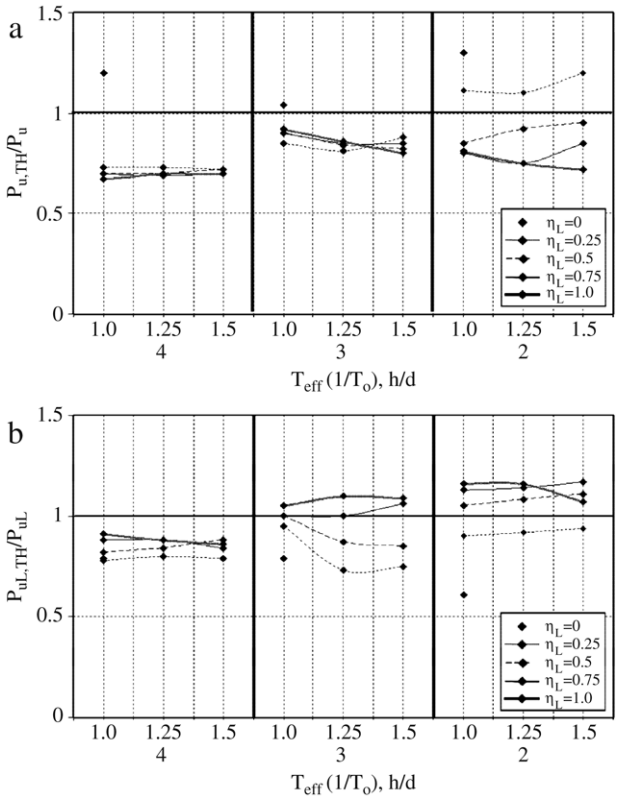

Fig. 7. Parametric study results (a) Normalized horizontal base shear results and (b) Normalized leg axial force results.

9.1. Results

Results of the parametric study show that the concepts presented predict maximum demands conservatively in all cases and with reasonable accuracy, with the some exceptions. The predicted maximum base shear of the free-rocking system ($\eta_L = 0$) is unconservative in all cases, underpredicted by approximately 18% on average, and 30% in the worst case considered. The predicted maximum leg axial forces are slightly unconservative (i.e. 17% at most) for $h/d = 2$ and most strength ratios. For greater conservatism, an absolute sum combination rule might be considered (mostly for the braces frames having smaller aspect ratios), but this was not investigated here as the results were deemed to be satisfactory for practical purposes.

10. Conclusions

The response of controlled rocking steel braced frames was investigated in an effort to quantify the dynamic effects that occur as a result of impacting and uplifting from the frame's support. The transition of the axis of rotation from the base of one leg to another followed by uplift is critical during the rocking response in terms of maximum dynamic forces developed in the frame. The excitation of vertical modes of vibration can cause significant vertical transient response even when the frame is subjected solely to horizontal ground motions.

Two significant modes of dynamic response involve axial vibration of a frame leg and vertical shearing deformations of the entire frame. The excitation of these modes was quantified here using simplified linear–elastic mass–spring models subjected to loading in the form of an initial velocity and impulsively applied loads. Methods to predict the maximum dynamic forces were developed and combination rules applied to account for the phase differences of individual dynamic effects. An example was presented for a frame representative of a bridge steel-truss pier with an aspect ratio of 4 to further illustrate the concepts discussed and nonlinear time history analysis was used to verify results of the example problem. A parametric study was then conducted to validate the concepts over a broader range of representative examples and the response of controlled rocking frames predicted by the proposed simplified procedures were compared with the results of nonlinear time history analyses. Results show that the concepts presented are reasonably accurate and simple enough to be used for design.

Acknowledgments

This research was supported in part by the Federal Highway Administration under contract number DTFH61-98-C-00094 to the Multidisciplinary Center for Earthquake Engineering Research. However, any opinions, findings, conclusions and recommendations presented in this paper are those of the authors and do not necessarily reflect the views of the sponsors.

References

[1] Pollino M, Bruneau M. Seismic retrofit of bridge steel truss piers using a controlled rocking approach. J Bridge Eng ASCE 2007;12(5):600–10.
[2] Housner G. The behavior of inverted pendulum structures during earthquakes. Bull Seismol Soc Amer 1963;53(2):403–17.
[3] Meek JW. Effects of foundation tipping on dynamic response. J Struct Div, ASCE 1975;101(ST7):1297–311.
[4] Psycharis IN. Dynamic behavior of rocking structures allowed to uplift, Ph.D. dissertation. Pasadena (CA): California Institute of Technology; 1982.
[5] Priestley MJN, Evison RJ, Carr AJ. Seismic response of structures free to rock on their foundations. Bull New Zealand National Soc Earthquake Eng 1978;11(3).
[6] Midorikawa M, Azuhata T, Ishihara T, Wada A. Shaking table tests on rocking structural systems installed yielding base plates in steel frames. In: Behaviour of steel structures in seismic areas. 2003. p. 449–54.
[7] Ajrab J, Pekcan G, Mander J. Rocking wall-frame structures with supplemental tendon systems. J Struct Div ASCE 2004;130(6):895–903.
[8] Dowdell D, Hamersley B. Lions' gate bridge north approach: Seismic retrofit. In: Behaviour steel structures in seismic areas: Proceedings of the third international conference. 2001. p. 319–26.
[9] Jones M, Holloway L, Toan V, Hinman J. Seismic retrofit of the 1927 carquinez bridge by a displacement capacity approach. In: Proceedings of the second national seismic conference on bridges and highways: Progress in research and practice. 1997.
[10] Prucz Z, Conway WB, Schade JE, Ouyang Y. Seismic retrofit concepts and details for long-span steel bridges. In: Proceedings of the 2nd national seismic conference on bridges and highways: Progress in research and practice. 1997.
[11] Ingham T, Rodriguez S, Nadar M, Taucer F, Seim C. Seismic retrofit of the golden gate bridge. In: Proceedings of the national seismic conference on bridges and highways: Progress in research and practice. 1997.
[12] Clough RW, Penzien J. Dynamics of structures. New York: McGraw-Hill, Inc; 1975.
[13] Newmark N, Hall W. Earthquake spectra and design. Oakland (CA): Earthquake Engineering Research Institute; 1982.
[14] ATC/MCEER, NCHRP 12-49 Recommended LRFD guidelines for the

seismic design of highway bridges, part I: Specifications, ATC/MCEER Joint Venture. 2003.
[15] Wen YK. Method for random vibration of hysteretic systems. J Eng Mech Div, ASCE 1976;102(EM2).
[16] Deodatis G. Non-stationary stochastic vector processes: Seismic ground motion applications. Prob Eng Mech 1996;11:149–67.